Analysis Of Laminar Flow Through A 3-D Geometry With Baffle's Of Different Size For Controlling Generation Of Recirculation Bubbles

RAJAT KABIRAJ[1], RANAJIT MIDYA[2], SNEHAMOY MAJUMDER[3]
[1, 2, 3] *Department of Mechanical Engineering, Jadavpur University, Kolkata, India*

Abstract- ***The research work presented here is the analysis of laminar fluid flow through a three dimensionl rectangular duct with baffles fitted at the lower wall, extending from one vertical wall to the other vertical wall respectively. The governing equations include the laminar Naviers Stokes eqution in a 3-D geometry neglecting body forces. The numerical methodology applied is the Control Volume Formulation of S. V. Patankar using SIMPLER Algoritham and power law scheme utilising the staggered grid conception. The results presented are the velocity vectors for different cases analysed along with the velocity, friction factor distributions. The streamtraces have been presented to visualize the recirculation bubble which is further corroborated by the presentation of the recirculation dimensions for different cases studied. It has been observed that both axial and vertical extent of the recirculation bubbles before and after bubbles strongly depends on buffle geometry and size. Though the variation are different for recirculation bubbles before and after the baffle respectively.***

Index Terms- ***3-D Rectangular duct, Laminar Flow, Control volume formulation, baffle, Recirculation bubble.***

NOMENCLATURE

x, y, z	Three dimensional coordinates, m
ϕ	Any variable
t	time, s
U_{in}	Velocity at Inlet, m/s
u	Velocity along x-axis, m/s
v	Velocity along y-axis, m/s
w	Velocity along z-axis, m/s
μ	Viscosity of the fluid, N-s/m^2
ρ	Density of the fluid, Kg/m^3
P	Pressure, N/m^2
L_X	Axial length of the geometry, m
L_Y	Length of the geometry in y-direction, m
L_Z	Length of the geometry along Z-axis, m
H	Height of the baffle, m
Recl	Recirculation bubble length, m
Recb	Recirculation bubble width, m
C_f	Fric coefficient
ν	Molecular kinematic Viscosity, m^2/s

I. INTRODUCTION

The laminar flow is encountered almost all engineering applications like the flow of fluid through duct, flow through river streams or atmospheric flows etc. Inman [1] have done an analysis to estimate convection heat transfer to slug flow in rectangular channel with uniform heat source in the field for a rectangular channel with heat generation in fluid stream. The results are applied in the thermal entrance as well as in the fully developed region and used for estimating local heat transfer characteristics when the Peclet number is approximately 100. Launder *et al*. [2] presents the outcome of experimental research on turbulence induced secondary flows in a square section duct. The main emphasis of the experiments has been on the measurement of the secondary flows in a duct with equally roughed surface. Melling *et al*. [3] done a detailed experimental study of developing turbulent flow in a rectangular duct using a laser-Doppler Anemometer. The contours of axial mean velocity turbulence intensity were measured in the developing flow. Demuren *et al* [4] have studied the flow in straight non-circular ducts involving turbulence-driven secondary motion. Doormaal *et al* [5] used SIMPLE method of Patankar and Spalding to solve the problems regarding incompressible flows. Molki & Mostoufizadeh [6] in his experiment investigated the heat transfer in rectangular ducts with repeated baffle blockages. The arrangements of the baffles are kept in a staggered fashion with fixed axial spacing. The presence of baffles enhances the heat transfer coefficients which are evaluated in the periodic fully developed and entrance region of the duct. Ravi and Vanka. [7] analysed the fully developed flow in a straight duct of square cross section by using the LES technique. Yang & Shiht.

[8] used the $\kappa-\varepsilon$ model for near wall turbulent flows. Hussert & Biringen. [9] in a study with a time splitting method by using numerical approach to integrate the 3-D incompressible Navier-stokes equations using spectral/high-order finite difference discretization on a staggered mesh. Wilcox [10] compared results between the low Reynolds number $\kappa-\varepsilon$ model and $\kappa-\omega$ model for high Reynolds number, incompressible, turbulent boundary layers with favourable, zero and adverse pressure gradient respectively.Srinath and Han [11] , Akira *et al.* [12] and Majumder and Sanyal [14] have performed the study of flow theoretically while Leschziner and Rodi [13] made the stream line bending correction in their modelling. Ali *et al* [15]. performed laminar flow analysis. In this paper we studied a 3-D laminar flow with baffle which is least addressed in researchers.

II. MATHEMATICAL FORMULATION

The axial length is 1.1 m, the other two dimensions are each 0.5 m, while two baffles are considered and the dimensions are 0.125 m and 0.250 m respectively, having width 0.1 m each one. The inlet flow is uniform with the Reynolds number of 750 width U_{in} =0.25 m/s and air as the working fluid.

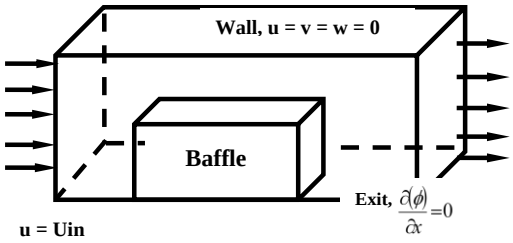

Fig. 1,The physical geometry and flow coniguration of the horizontal rectangular duct

Governing Equations
Continuity Equation:

$$\frac{\partial u}{\partial x}+\frac{\partial v}{\partial y}+\frac{\partial w}{\partial z}=0 \qquad (1)$$

X-momentum equation:

$$\frac{\partial u}{\partial t}+u\frac{\partial u}{\partial x}+v\frac{\partial u}{\partial y}+w\frac{\partial u}{\partial z}=-\frac{1}{\rho}\frac{\partial p}{\partial x}+\upsilon\left[\frac{\partial^2 u}{\partial x^2}+\frac{\partial^2 u}{\partial y^2}+\frac{\partial^2 u}{\partial z^2}\right] \quad (2)$$

Y-momentum equation

$$\frac{\partial v}{\partial t}+u\frac{\partial v}{\partial x}+v\frac{\partial v}{\partial y}+w\frac{\partial v}{\partial z}=-\frac{1}{\rho}\frac{\partial p}{\partial x}+\upsilon\left[\frac{\partial^2 v}{\partial x^2}+\frac{\partial^2 v}{\partial y^2}+\frac{\partial^2 v}{\partial z^2}\right] \quad (3)$$

Z-momentum equation

$$\frac{\partial w}{\partial t}+u\frac{\partial w}{\partial x}+v\frac{\partial w}{\partial y}+w\frac{\partial w}{\partial z}=-\frac{1}{\rho}\frac{\partial p}{\partial x}+\upsilon\left[\frac{\partial^2 w}{\partial x^2}+\frac{\partial^2 w}{\partial y^2}+\frac{\partial^2 w}{\partial z^2}\right] \quad (4)$$

Boundary Conditions
Inlet

u = Uin, v=0, w=0

Walls :No slip boundary conditions

U = V = W = 0

EXIT

$\frac{\partial(\phi)}{\partial x}=0$, (Fully developed condition),

Where $\phi = U \ or \ V \ or \ W \ etc.$

The dimensionless forms are interpreted as follows:
$X = x / D_{h;}$ $Y = y / D_h$;$Z = z / D_h$;
$U = u / U_{in}$; $V = v/U_{in}$; $W = w/U_{in}$

III. SOLUTION METHODOLOGY

The mathematical formulations and models described above consist of sets of differential equations subjected to appropriate boundary conditions. To provide the algebraic form of the governing equations, a fully staggered grid system have been adopted for the velocity components and the scalar variables and these equations were discretized using a control volume formulation. The vectors are solved at the control volume boundary surface while the scalar quantities are solved at the cell centre. The numerical solution in the present work is accomplished by using Semi implicit method for pressure linked equation revised (SIMPLER) and the power-law scheme proposed by S. V. Patankar.

IV. RESULTS AND DISCUSSION

Grid Independent Study and Validation
For the authenticity of the computer code the grid independence studuy has to be performed. A grid

independence study has been performed with two grid sizes 151 x 21 x 81 and 71 x 11 x 41 and it has been found that the results almost collapse on each other. Hence the second grid system has been adopted throughout the calculation. A typical grid structure with uniform grid generation has been shown in the figure 2 for the purpose of understanding the complicacy with 3-D flow analysis indicating the requirement of the computational platform required in a turbulent 3-D flow. While the validation study shows a deviation of less than 0.1%. with benchmark solution. The exit velocity profile for simple 3-D geometry for a laminar flow is flat in core region as shown in the figure 3 indicating the authenticity of the numerical method adopted and disturbed flow due to the pressure of baffle.

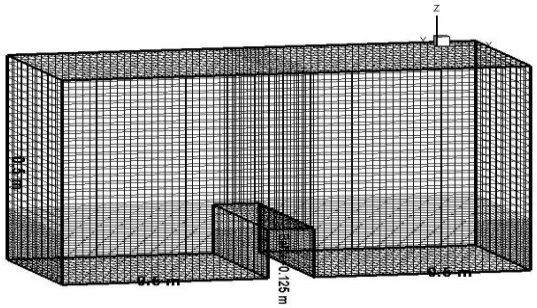

Fig. 2, Typical 3-D grid required for the solution of three dimensional turbulent flow.

In the figure 4 it is observed that there are presence of recirculation bubbles with different strength at the preceding region of the baffle as well as at the immediate after the baffle respectively. They are three dimensional in nature and they are produced due to the fact that there is a adverse pressure gradient generated at those regions for which the detachment of the flow occurs with reversal of the velocity. These are low pressure zones where reattachment point resides usually near the or at the top portion of the baffle. The region above the baffle is receving full discharge and there the flow is accelerated due to the reduction in cross section of the flow, however though there must be a smaller recirculation bubble at the op most of the baffle but it is not very eminent atleast for this baffle size of 0.125 m used at this diagram.

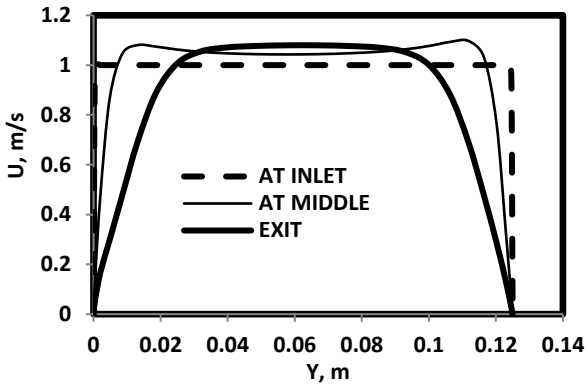

Fig. 3, Velocity profile for simple 3-D rectangular geometry.

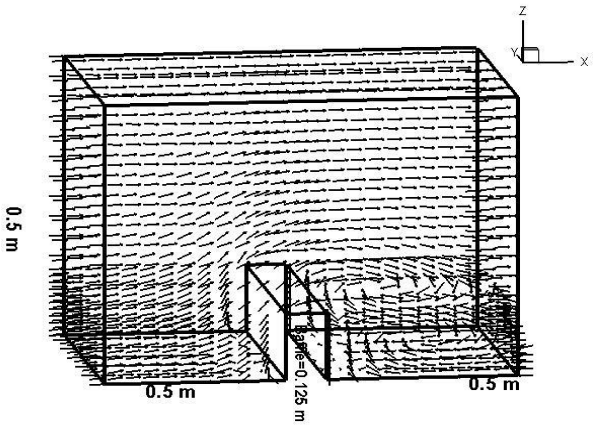

Fig.4, Velocity vector in the 3_D geometry shoing the recirculating zones.

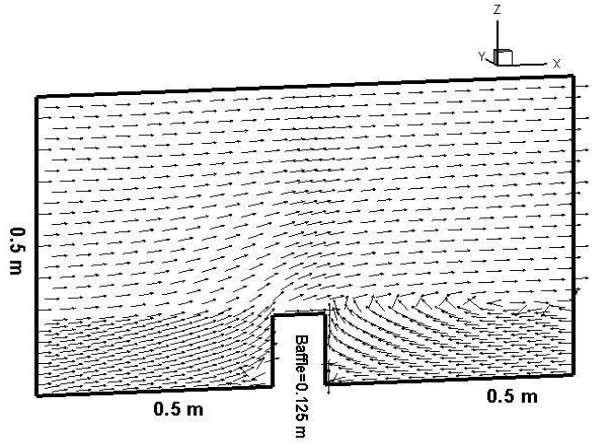

Fig. 5, Velocity Vector in the mid axial plane for baffle size of 0.125 m.

The flow visualisation at the figure 5 at the mid axial plane corroborates these findings already explained in connection with the figure 4. Here the recirculations are very prominent and the bending of the streamline is also very clear. At this diagram a flavour of the tiny recirculation at the top of the baffle is felt though obscure in presence. The same analysis is also true for the same plane with the stream traces as shown in the figure 6. Figure 7

shows the velocity distributions before the baffle and here the flow reversal is revealed by the negative velocity field present near the lower wall. The sharp velocity gradient is associated with the separating flow at this region.

Figure 8 represents the velocity vector in the 3-D geometry but for different height of the baffle. In this case the flow configuration is grossly same only the recirculation strength increase owing to the change of boundary conditions i.e. the baffle height has increased. Consequently the flow negotiation along and over the baffle is more so the reattachment length and breadth is also enhanced. There is a tiny secondary recirculation bubble on the top of the baffle. This is clearly visible in the figures 9 and 10 respectively. Figure 10 reveals this very lucidly. Though this secondary recirculation bubble is tiny in size but it has great influence, because it further narrowdown the flow area above the baffle and consequently acceleration of the flow over the baffle increases.

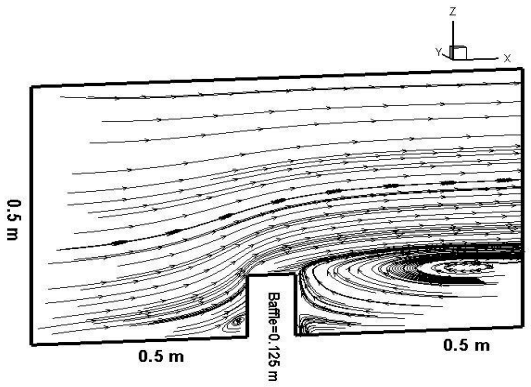

Fig. 6, Stream traces at the mid plane for baffle size of 0.125 m

Figure 11 shows the velocity field which clearly shows that the flow reversal zone is more indicating the strength of the recirculation bubble to be more. Figure 12 shows the friction factor variation at the upper wall for both of the baffles. Here we can see that for the higher value of baffle height the friction factor is more. This is because the restriction of flow blockage by the baffle is more. Finally figures 13 and 14 represents the recirculation bubble length before and after the baffle. The distribution also gives the correlation as depicted in the figures. These correlation it is possible to estimate the recirculation strength roughly

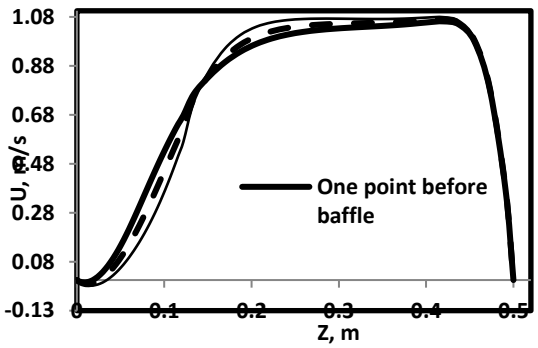

Fig. 7, Velocity distribution before the baffle for baffle size of 0.125 m.

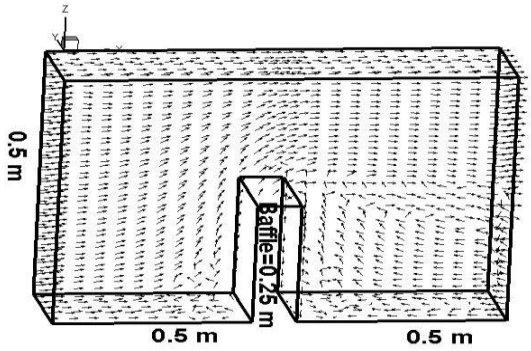

Fig. 8, Velocity vector in the 3_D geometry shoing the recirculating zones

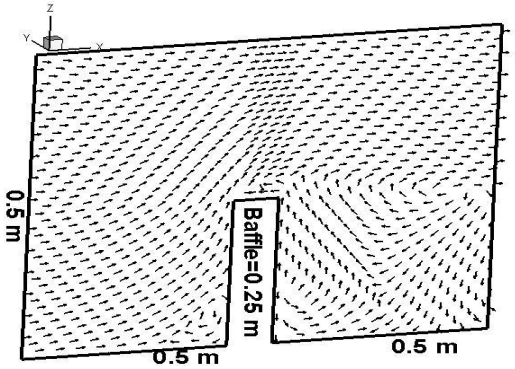

Fig. 9, Velocity Vector in the mid axial plane for baffle size of 0.25 m.

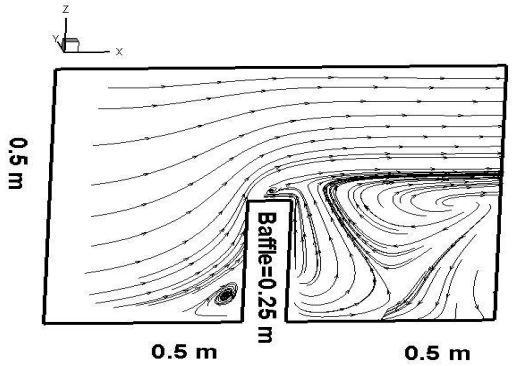

Fig. 10, Stream traces at the mid plane for baffle size of 0.25 m

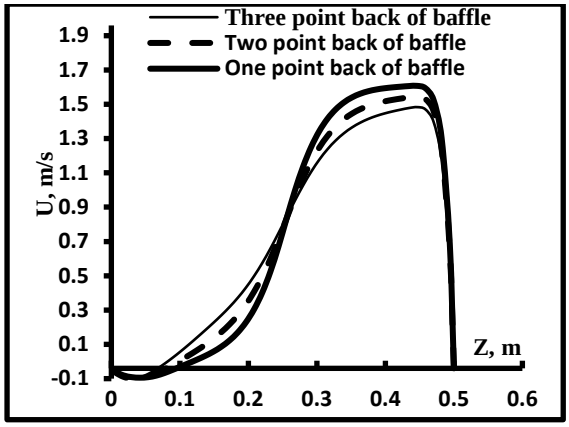

Fig. 11, Velocity distribution before the baffle for baffle size of 0.25 m.

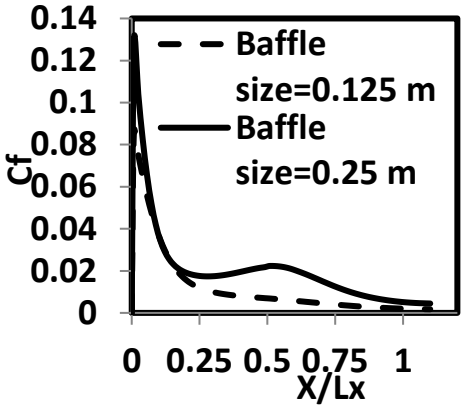

Fig. 12, Friction factor distributions.

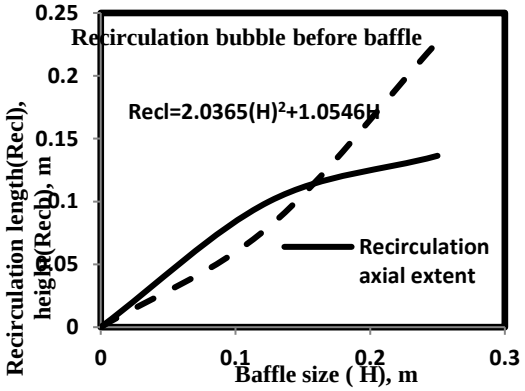

Fig. 13, Recirculation bubble dimensions and correlations before the baffles.

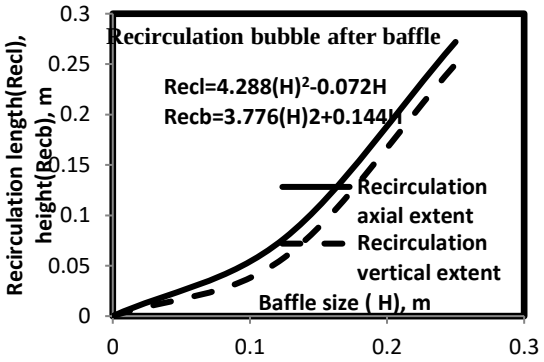

Fig. 14, Recirculation bubble dimensions and correlations after the baffles.

CONCLUSION

A numerical analysis of turbulent fluid flow through a 3-D geometry with baffle has been carried out. The presence of recirculation or separating flow is confirmed. With the increase in baffle the recirculation strength increases. The Friction factor is more for the higher size of the baffle. With the increase of size of the baffle the recirculation bubble over the baffle increases.

REFERENCES

[1]

[1] Robert M. Inman, 1967 'Heat-transfer analysis for liquid-metal flow in rectangular channels with heat sources in the fluid'*National aeronautics and space administration*, February 1967.

[2] B. E. Launder And W. M. Ying, 1972, 'Secondary flows in ducts of square cross-section' *J .Fluid Mech., vol.* 54, *part* 2, *pp.* 289-295.

[3] A. Melling And J. H. Whitelaw, 1976, 'Turbulent flow in a rectangular duct, *J. Fluid Mech., vol.* 78, *part* 2, *pp.* 289-315

[4] A. O. Demuren And W. Rodi, 1983, 'Calculation of turbulence-driven secondary motion in non-circular ducts', *Fluid Mech., vol.* 140, *pp.* 189-222.

[5] J. P. Van Doormaal and G. D. Raithby,1984,'Enhancements of the SIMPLE method for predicting incompressible fluid flows', *Numerical Heat Transfer*, vol. 7, pp. 147-163.

[6] M. Molki and A. R. Mostoufizadeh, 1988, 'Turbulent heat transfers in rectangular ducts with repeated-baffle blockages', *Int. J. Heat Mass Transfer.*, Vol. 32, No. 8, pp. 1491-1499.

[7] Ravi K. Madabhushi and S. P. Vanka, 1991 'large eddy simulation on turbulence-driven secondary flow in square duct', *Department of Mechanical and Industrial Engineering, University of Illinois at Urbana-Champaign, Urbana, Illinois*, 6180I.

[8] Z.Yang and T. H. Shiht,1993,'New Time Scale Based $\kappa - \varepsilon$ Model for Near-Wall Turbulence', *AIAA JOURNAL*, 1993, Vol. 31, No. 7, July.

[9] Asmund Husert And Sedat Biringen, 1993, 'Direct numerical simulation of turbulent flow in a square duct', *J. Fluid Mech., vol.* 257, *pp.* 65-95

[10] David C. Wilcox, 1993, 'Comparison of Two-Equation Turbulence Models for Boundary Layers with Pressure Gradient' *AIAA JOURNAL,* August 1993, Vol. 31, No. 8.

[11] Srinath V. Ekkadand J. E-Chin Han, 1996, 'Detailed heat transfer distributions in two-pass square channels with rib turbulators', *Int. J. Heat Mass Transfer,* 1997, Vol. 40, No. 11, pp. 2527-2537.

[12] Akira Murataa, Sadanari Mochizuki, Tatsuji Takahashi, 1999, 'Local heat transfer measurements of an orthogonally rotating square duct with angled rib turbulators', *Columbia International Publishing American Journal of Heat and Mass Transfer,* 1999, 42, 3047-3056

[13] M. A. Leschziner and W. Rodi, *Calculation of Annular and Twin Parallel Jets Using Various Discretization Schemes and Turbulence-Model Variations,*Trans. ASME, J. Fluids Engg. 103(1981), pp. 352-360.

[14] S. Majumder, and D.Sanyal, *Destabilization of Laminar Wall Jet Flow and Re-Laminarization of the Turbulent Confined Jet Flow in Axially Rotating Circular Pipe,*Trans.ASME, Journal of Fluids Engg.130 (2008),pp. 011203-1 – 011203-8.

[15] A. Ali, M Asif Memon, and A. Majed Albugami, 2021, 'Numerical analysis of laminar flow and heat transfer through a rectangular channel containing perforated plate at different angles. Energy Reports 8(1):539-550.